
EVALUATING MASSIVELY PARALLEL ALGORITHMS FOR DFA MINIMISATION, EQUIVALENCE CHECKING AND INCLUSION CHECKING

JAN HEEMSTRA^a, JAN MARTENS^b, AND ANTON WIJS^a

^a Eindhoven University of Technology, The Netherlands
e-mail address: j.h.heemstra@tue.nl, a.j.wijs@tue.nl

^b Leiden University, The Netherlands
e-mail address: j.j.m.martens@liacs.leidenuniv.nl

ABSTRACT. We study parallel algorithms for the minimisation and equivalence checking of Deterministic Finite Automata (DFAs). Regarding DFA minimisation, we implement four different massively parallel algorithms on Graphics Processing Units (GPUs). Our results confirm the expectations that the algorithm with the theoretically best time complexity is not practically suitable to run on GPUs due to the large amount of resources needed. We empirically verify that parallel partition refinement algorithms from the literature perform better in practice, even though their time complexity is worse. Furthermore, we introduce a novel algorithm based on partition refinement with an extra parallel partial transitive closure step and show that on specific benchmarks it has better run-time complexity and performs better in practice.

In addition, we address checking the language equivalence and inclusion of two DFAs. We consider the Hopcroft-Karp algorithm, and explain how a variant of it can be parallelised for GPUs. We note that these problems can be encoded for the GPU-accelerated model checker GPUEXPLORE, allowing the use its lockless hash table and fine-grained parallel work distribution mechanism.

1. INTRODUCTION

In contrast to sequential chips, the processing power of parallel devices keeps increasing. Graphics Processing Units, or GPUs, are examples of such devices. Originating from the need to do simple computations for many (independent) pixels to generate graphics, GPUs have also shown useful as computational powerhouses, and led to general-purpose computing on GPUs (GPGPU). Most convincingly, GPUs have become indispensable in training models for artificial intelligence. Because of the enormous potential of GPUs, it is important to investigate how computational problem solving can be accelerated with them.

Deterministic Finite Automata (DFAs) are one of the simplest computational formalisms. The natural problem of computing a minimal machine that is equivalent to a given machine w.r.t. the input is omnipresent in the field of theoretical computer science. In the case of

Key words and phrases: GPU, DFA minimisation, parallel minimisation, DFA equivalence checking, parallel equivalence checking.

DFAs the problem has a rich history. The first method that computes a minimal DFA dates back to Moore’s framework [Moo56], and is a *partition refinement* algorithm. Later, this algorithm was adapted by Hopcroft [Hop71] to a quasi-linear time algorithm.

The complexity class known as Nick’s Class (NC) consists of the problems that can be solved in polylogarithmic time with a parallel machine using a polynomial number of parallel processors. It is an open question whether $NC \stackrel{?}{=} P$, but it is widely believed that this is not the case. Similar to the assumption that decision problems not in P are inherently difficult (known as Cobham’s thesis), we can think of P -complete problems as being inherently sequential.

The problem of minimizing DFAs is known to be in NC [CH92], which intuitively means it can be efficiently computed in parallel. In contrast, the problem of computing bisimilarity on non-deterministic structures is known to be P -complete [BGS92]. Interestingly, the most efficient sequential algorithms for these two problems, i.e., Hopcroft’s algorithm [Hop71] and an algorithm based on Paige-Tarjan [PT87], respectively, are very similar. In particular, these algorithms are both *partition refinement* algorithms.

The parallel algorithms studied for computing bisimilarity on non-deterministic structures and DFA minimisation are also partition refinement algorithms [MGH⁺22, RX96, TSG02, Wij15]. Since DFA minimisation is in NC , there is a parallel sublinear time algorithm. However, none of these partition refinement algorithms studied have a sublinear run-time. A linear lower bound for the parallel run-time was proven in [GMdV23] for any parallel partition refinement algorithm deciding bisimilarity, and this result also directly applies to deterministic structures such as DFA minimisation. This means that no partition refinement algorithm can achieve the theoretically optimal run-time on parallel machines. It is therefore interesting to investigate whether there is an algorithm that is not a partition refinement algorithm that performs better in parallel than partition refinement algorithms.

The algorithm introduced in [CH92] runs in logarithmic time. However, the work is mainly theoretical and the large amount of parallel processors and memory required makes it unlikely to scale well in practice. The main constraint here is the need to compute the transitive closure for the underlying graph of the DFA. It seems hard to find a significant improvement in the number of parallel processors needed.

In this article, we compare implementations of different parallel algorithms for DFA minimisation on GPUs, using the various parallel algorithms proposed in the literature as a basis. This comparison can be found in Section 3. We establish that the logarithmic runtime complexity with the construction from [CH92] is not feasible due to the large amount of processors needed. Additionally, we find that on our benchmarks, described in Section 5, the partition refinement algorithm that uses sorting in each iteration performs better than the naive splitting strategy on the more diverse benchmarks from the VLTS benchmark set,¹ but worse for benchmarks that are known to be hard for partition refinement algorithms. Finally, we show a method of adding a partial transitive closure as a preprocessing step that can significantly increase the performance on benchmarks with a very specific shape.

This article is based on a previously published paper [MW24]. While the work on DFA minimisation stems from that earlier publication, the current article extends the scope by also considering equivalence checking and inclusion checking of DFAs, two other fundamental operations that have their practical use in applications such as model checking and compiler construction. A well-known algorithm for DFA equivalence checking is the algorithm by

¹<https://cadp.inria.fr/resources/vlts> (visited on: 19-04-2024).

Hopcroft and Karp [HK71, AHU74]. Its almost linear complexity is due to the fact that the algorithm constructs the transitive closure of a bisimulation relation using a union-find data structure. Although this is hard to achieve in a massively parallel way, we show that a naive version of the algorithm, in which the bisimulation relation is constructed using a hash table, but its transitive closure is not explicitly maintained, works well in practice. To achieve this, in Section 4, we use the GPU-accelerated explicit-state model checker GPUEXPLORE [WO23a, WO24], which contains all the ingredients to encode the problem of DFA equivalence checking, and perform the computations on the GPU. To demonstrate the effectiveness of this approach, we define some additional benchmarks, and report on the results obtained with these benchmarks, in Section 5. The naive version of the algorithm by Hopcroft and Karp can also be used for inclusion checking, i.e., checking that the language of one DFA is included in the language of another DFA. Also for this operation, we explain how to encode this for GPUEXPLORE, perform experiments and discuss the performance of our approach.

Finally, in Section 6, we draw conclusions and provide pointers for future work.

2. PRELIMINARIES

We write $\mathbb{B} = \{\mathbf{true}, \mathbf{false}\}$ for the set of booleans, \mathbb{N} for the set of natural numbers, and for numbers $i, j \in \mathbb{N}$ we define $[i, j] = \{c \in \mathbb{N} \mid i \leq c \leq j\} \subseteq \mathbb{N}$, the closed interval from i to j . Given an alphabet Σ , a sequence $a_1 a_2 \dots a_n$ of symbols from Σ is called a word. We write Σ^* for the set containing all finite sequences of letters in Σ . The empty-sequence consisting of no symbols is written as ε .

Definition 1. (Deterministic Finite Automaton) A deterministic finite automaton (DFA) $A = (Q, \Sigma, \delta, F, q_0)$ is a five-tuple consisting of:

- a finite set of states Q ,
- a finite alphabet Σ ,
- a transition function $\delta : Q \times \Sigma \rightarrow Q$,
- a set of accepting states $F \subseteq Q$, and
- an initial state $q_0 \in Q$.

We sometimes write $q \xrightarrow{a} q'$ if $\delta(q, a) = q'$. The function $\delta^* : Q \times \Sigma^* \rightarrow Q$ extends the transition function to words and is defined inductively for all words in Σ^* as follows:

$$\begin{aligned} \delta^*(q, \varepsilon) &= q \\ \delta^*(q, aw) &= \delta^*(\delta(q, a), w) \end{aligned}$$

Given a DFA $A = (Q, \Sigma, \delta, F, q_0)$, a word $w \in \Sigma^*$ is *accepted* iff $\delta^*(q_0, w) \in F$. The language of a DFA A , notation $\mathcal{L}(A)$, is the set of all words $w \in \Sigma^*$ that are accepted by A .

We consider the problem of computing the minimal DFA, i.e., given a DFA A , identifying the DFA A' with the smallest number of states such that $\mathcal{L}(A') = \mathcal{L}(A)$.

Minimizing DFAs consists of combining undistinguishable states and deleting unreachable states. The main part of the problem consists of combining states, and removing unreachable states can be seen as a simple pre-processing step. For the remainder of the paper, we assume that all the states in a DFA are reachable from its initial state. The algorithms can be seen as computing bisimilarity, or the coarsest set partition problem, without the preprocessing step that removes unreachable states.

Representation. For an input automaton $A = (Q, \Sigma, \delta, F, q_0)$, we assume that the states in Q and letters in Σ are represented by unique indices, i.e., $Q = \{0, \dots, |Q|\}$ and $\Sigma = \{0, \dots, |\Sigma|\}$. The transition function δ is represented by $|\Sigma|$ arrays of length $|Q|$, such that for state $q \in Q$ and letter $a \in \Sigma$, $\delta[a][q] = \delta(q, a)$.

The PRAM Model. The complexities we mention assume the model of the *Parallel Random Access Machine (PRAM)*. The PRAM is a natural extension of the RAM model, where parallel processors have access to a shared memory. A PRAM consists of a sequence of processors P_0, P_1, \dots and a function \mathcal{P} that given the size of the input defines a bound on the number of processors used.

Each processor P_i has the natural instructions of a normal RAM and in addition has an instruction to retrieve its unique index i . All processors run the same program in lock-step, using their index to identify the data they need to access. This parallel processing is called single-instruction multiple data (SIMD).

There are many different ways to handle data-races. We assume the concurrent read, concurrent write (CRCW) model following [SV84], where processors are allowed to read from and write to the same memory location concurrently. After multiple concurrent writes to the same memory location, that location contains the result of one of those writes.

GPUs. While in reality, no device completely adheres to the PRAM model, recent hardware advancements has led to devices that are getting better and better at approximating this model. The GPU, in particular, is a very suitable target platform for PRAM algorithms, as it has been specifically designed for SIMD processing. The performance of GPU programs typically relies on launching tens to hundreds of thousands of threads, as the performance of these programs is often memory-bound: accessing the input data in the GPU's *global* memory, in NVIDIA CUDA terminology, is relatively slow. This latency can be hidden by a GPU via fast context switching between threads. As one thread is waiting for data to be retrieved, another thread is executed in the meantime on the same processor. It is this fast context switching between threads that allows GPUs, typically equipped with several thousands of cores, to virtually execute hundreds of thousands of threads concurrently. In the current work, we employ NVIDIA GPUs, programs for which can be written in CUDA C++.

3. ALGORITHMS FOR DFA MINIMISATION

3.1. Transitive closure. The first algorithm we discuss for DFA minimisation has theoretical polylogarithmic runtime [CH92]. However, the large amount of memory and parallel processors it uses makes it unlikely to work in practice. Here we confirm this fact.

The idea is rather simple; build a graph with nodes $V = Q \times Q$ and edges E containing $(q, q') \rightarrow (p, p')$ iff there is a letter $a \in \Sigma$ such that $\delta(q, a) = p$ and $\delta(q', a) = p'$. Initially, in the array **Apart** we label the nodes $(q, q') \in V$ to be inequivalent if $q \in F \iff q' \notin F$. Any two states $q, q' \in Q$ are not equivalent iff they were initially labelled in **Apart** or there is a path to a labelled node. Computing this reachability of false nodes can be seen as computing the transitive closure in the directed graph (V, E) containing n^2 nodes. In parallel this computation can be done in polylogarithmic running time using $O(|V|^3)$ parallel processors [J92, Chapter 5.5.].

Algorithm 1, which we refer to as **trans**, implements this idea. First, at lines 4–7 (l.4–7), the graph is constructed, inequivalent nodes labelled in the *Apart* data structure and the

Algorithm 1 Transitive DFA minimisation **trans**.**Input:** A DFA $A = (Q, \Sigma, \delta, F, q_0)$ where $|Q| = n$ **Output:** The minimal quotient automaton represented in the matrix $Apart$

```

1:  $V :: Q \times Q$  ▷ Nodes of graph consisting of pair of states
2:  $Apart :: \text{Array}[n^2]$  of type  $\mathbb{B}$ 
3:  $Reach :: \text{Array}[n^2][n^2]$  of type  $\mathbb{B}$  ▷ Represents reachability in  $V$ , initially false
4: do in parallel for  $(q, q') \in V$  ▷ Initializes data structures in parallel.
5:    $Apart[(q, q')] := (q \in F \iff q' \notin F)$  ▷ State initially unequal
6:   for all  $a \in \Sigma$  do
7:      $Reach[(q, q')][(\delta(q, a), \delta(q', a))] := \text{true}$ 
8:  $stable := \text{false}$ 
9: while  $\neg stable$  do
10:    $stable := \text{true}$ 
11:   do in parallel for  $s, t, u \in V$ 
12:     if  $Reach[s][t]$  and  $Reach[t][u]$  and  $\neg Reach[s][u]$  then
13:        $Reach[s][u] := \text{true}$ 
14:   do in parallel for  $s, t \in V$ 
15:     if  $Reach[s][t]$  and  $Apart[t]$  and  $\neg Apart[s]$  then
16:        $Apart[s] := \text{true}$ 
17:    $stable := \text{false}$ 

```

edges stored in the adjacency matrix $Reach$. Next, the parallel transitive closure of $Reach$ is computed and $Apart$ updated accordingly. If in an iteration there is no new pair of states labelled $Apart$ the algorithm is finished. The minimal automaton is represented in the graph where states $q, q' \in Q$ can be combined if $\neg Apart(q, q')$.

Computing the transitive closure for a directed graph in logarithmic time requires many processors. Our naive implementation requires $|V|^3$ parallel processors. Given a DFA with n states, this means that since $|V| = n^2$, we require n^6 processors. Theoretically, more efficient methods are known for computing the transitive closure, which uses matrix multiplication. Matrix multiplication can be computed with $O(n^\omega)$ operations, where currently $\omega \leq 2.372 \dots$, this means we can compute our transitive closure with $O(|V|^\omega)$ processors. Since these algorithms are non-trivial and already $|V| = n^2$, we believe these improvements would not significantly change the results mentioned here.

3.2. Naive partition refinement. The next algorithm for DFA minimisation, **naivePR**, is an adaptation of the parallel algorithm for bisimilarity checking of Kripke structures from [MGH⁺22]. The program runs on a PRAM with $\max(n, m)$ processes, where n is the number of states and $m = |\Sigma| * n$ is the number of transitions in the input DFA.

The algorithm applies *partition refinement*: states are initially partitioned into *blocks*, and the algorithm repeatedly splits blocks into smaller blocks until a fix-point is reached. Once this has happened, each block represents one state of the minimized DFA.

When splitting blocks in parallel, one particular challenge is how to identify newly created blocks, as each new block requires a unique identifier. Algorithm 2 does this by means of a leader election procedure: for each block, one of its states is elected leader, meaning that it is used as an identifier to refer to the block. In this way each iteration of the algorithm takes constant time if performed on a parallel machine that has concurrent writes.

In Algorithm 2, at l.1, an array *block* is initialized that defines for every state in Q its current block (as represented by a leader in Q). An array *new_leader* is defined at l.2 that is used to elect new leaders. At l.3, the initial leaders are selected: one state $q_f \in F$ for the block consisting of all the accepting states $q \in F$, and one state $q_n \in Q \setminus F$ for all the non-accepting states $q' \in Q \setminus F$. The array *block* is subsequently initialised using these leaders (l.4–5).

Next, partition refinement is applied inside the **while**-loop at l.7. The variable *stable* is used to monitor whether a fix-point has been reached, which has happened as soon as no blocks can be split any further. At the start of each iteration through the **while**-loop, *stable* is set to **true** (l.8). Next, all transitions of the DFA are processed in parallel (l.9), and for each transition $q \xrightarrow{a} q'$, it is checked whether *block*[q'] differs from the block that the leader *block*[q] can reach via an a -transition. If it does, then q should be separated from its leader. At l.11, q is assigned to *new_leader*[*block*[q]], the latter being the position where the leader for the new block will be elected. Here, the result of concurrent writes, as allowed by the PRAM CRCW model, is used for leader election.

Subsequently, when l.12 is reached, *new_leader* contains the newly elected leaders: specifically, at *new_leader*[*block*[q]], the leader for the new block created by splitting off states from *block*[q] is stored. In the parallel loop of l.12, the transitions are once more processed in parallel, and whenever a state turns out to differ from its leader regarding block reachability (l.13), the leader of that state is updated (l.14). Finally, since a block has been split, *stable* is set to **false** at l.15.

The largest difference between Algorithm 2 and the original algorithm [MGH⁺22] is that Algorithm 2 splits blocks directly w.r.t. the leader, as opposed to first selecting one particular block as *splitter*, and splitting those blocks in which some states differ w.r.t. their leader concerning the ability to reach the splitter. The reason for this difference is that for DFAs, comparing the outgoing transitions of two states is much more straightforward, as each state has exactly one outgoing transition for every $a \in \Sigma$. In the setting of LTSs, due to non-determinism it is not possible to directly compare the behaviour of a state with the leader state, and hence a fixed splitter is chosen before.

In Algorithm 2, leader election is performed in two phases: in the first phase (l.9–11), states are written to *new_leader* to elect new leaders, and the results are subsequently read at l.12–15. One could argue that this is inefficient, and that it would perhaps be better to combine these two phases. This is possible, but it requires the use of atomic *compare-and-swap* (CAS) operations. This is illustrated in Algorithm 3. In the single loop at l.11–17, new leaders are written to and read from *new_leader*. At l.14–15, the use of a compare-and-swap operation is described: in one atomic operation, the current value stored at *new_leader*[*leader*] is stored in *new_block*, and it is checked whether *new_leader*[*leader*] is equal to the initial value \perp , and if it is, it is set to q . Next, at l.16, if *new_block* is equal to \perp , it means q has been elected as leader. Otherwise, *new_block* indicates which state is the new leader. Note that for this to work, after execution of the loop at l.11, the values of *new_leader* have to be reset to \perp .

In practice, we experienced that a GPU implementation (in CUDA 12.2) of Algorithm 3 exhibits similar runtimes compared to a GPU implementation of Algorithm 2. The benefit of merging the loops seems to be negated by the use of atomic operations. For this reason, when discussing the experiments in Section 5.2, we do not involve Algorithm 3.

Algorithm 2 Parallel leader-election-based algorithm *naivePR*.

Input: A DFA $A = (Q, \Sigma, \delta, F, q_0)$ where $|Q| = n$
Output: The minimal quotient automaton represented in the array *block*

```

1: block :: Array[n] of type Q
2: new_leader :: Array[n] of type Q
3: Select initial leader states  $q_f \in F$  and  $q_n \in Q \setminus F$ 
4: do in parallel for  $q \in Q$ 
5:   block[q] := ( $q \in F$  ?  $q_f$  :  $q_n$ ) ▷ Initialize
6: stable := false
7: while  $\neg$ stable do
8:   stable := true
9:   do in parallel for  $q, a \in Q \times \Sigma$ 
10:    if block[ $\delta(q, a)$ ]  $\neq$  block[ $\delta(\text{block}[q], a)$ ] then
11:      new_leader[block[q]] := q ▷ Leader election
12:    do in parallel for  $q, a \in Q \times \Sigma$ 
13:      if block[ $\delta(q, a)$ ]  $\neq$  block[ $\delta(\text{block}[q], a)$ ] then
14:        block[q] := new_leader[block[q]] ▷ Split from leader
15:      stable := false

```

Algorithm 3 Parallel leader-election based *naivePR* with atomics.

Input: A DFA $A = (Q, \Sigma, \delta, F, q_0)$, where $|Q| = n$
Output: The minimal quotient automaton represented in the array *block*

```

1: block :: Array[n] of type Q
2: new_block :: Q
3: leader :: Q
4: new_leader :: Array[n] of type Q
5: Select initial leader states  $q_f \in F$  and  $q_n \in Q \setminus F$ 
6: do in parallel for  $q \in Q$ 
7:   new_leader[q] :=  $\perp$  ▷ Initialize
8:   block[q] := ( $q \in F$  ?  $q_f$  :  $q_n$ )
9: while  $\neg$ stable do
10:  stable := true
11:  do in parallel for  $q, a \in Q \times \Sigma$ 
12:    leader := block[q]
13:    if block[ $\delta(q, a)$ ]  $\neq$  block[ $\delta(\text{leader}, a)$ ] then
14:      { new_block := new_leader[leader]; ▷ Leader election with CAS
15:      new_leader[leader] =  $\perp$  ? new_leader[leader] := q }
16:      block[q] := new_block =  $\perp$  ? q : new_block ▷ Split from leader
17:      stable := false
18:  do in parallel for  $q \in Q$ 
19:    new_leader[q] :=  $\perp$ 

```

3.3. Sorting arrays. The next algorithm for DFA minimisation is an algorithm inspired by [RX96, TSG02]. Similar to Algorithm 2, this algorithm also performs partition refinement, but instead of doing so using leader elections, it repeatedly computes a *signature* for every

state, and sorts the states w.r.t. their signatures. This method allows splitting a block in more than two subblocks with the downside that each iteration takes more than constant parallel time.

The algorithm from [TSG02] uses hashing to construct and compare signatures. Since sorting arrays is a very native operation on GPUs, we follow [RX96] and use a sorting approach to construct the new blocks.

Algorithm 4 presents this approach as `sortPR`. Again, an array *block* is created (1.1). In addition, an array *state* is used for sorting the states (1.2). The signature of a state consists of a list of block IDs, one for each $a \in \Sigma$: *signature*[*q*][*a*] is equal to q' iff $q \xrightarrow{a} q''$ and *block*[q''] = q' .

The array *new_block* is used to store the results of assigning new blocks to states (1.4). Finally, the current number of blocks is stored at 1.5 in *num_blocks*.

Next, at 1.6–8, *block* and *state* are initialised. The block consisting of all accepting states is given ID 0, while the other states are assigned to block 1 (1.7). All the states are added to *state* at 1.8.

In the loop at 1.9–19, the partition refinement is performed until a fix-point has been reached, i.e., the number of blocks has not increased (1.19). In each iteration of this loop, the following is performed. First, in parallel, the signatures are updated (1.11–12). After that, *state* is sorted in parallel, using *signature* to compare states. The comparison function is given at 1.20–26. First, states are compared based on the block they reside in. If they reside in the same block, then the blocks they can reach via outgoing transitions are compared. Note that the for loop starting in (1.23) is sequential and requires iterating over the alphabet letters in a fixed order.

Once *state* has been sorted, the parallel *adjacent difference* is computed and stored in *new_block*. The result of this is that *new_block*[0] = *state*[0] and for all $0 < i < n$, *new_block*[*i*] = *are_neq*(*state*[*i*], *state*[*i* − 1]), with *are_neq* as defined at 1.27–31. Once *new_block*[0] has been reset to 0 (1.15), *new_block* contains only 0's and 1's, with each 1 identifying the start of a new block. At 1.16, an *inclusive scan* is performed in parallel, resulting in *new_block* having been updated in such a way that for each $0 \leq i < n$, *new_block*[*i*] = $\sum_{0 \leq j \leq i} \text{new_block}'[j]$, with *new_block'* referring to *new_block* at the start of executing 1.16.

Now, for all $0 \leq i < n$, *new_block*[*i*] contains the new block of state *state*[*i*]. At 1.17–18, *block* is updated in parallel to reflect this. As the largest new block ID can be found at *new_block*[*n* − 1], this location can be used to determine the new number of blocks at 1.19.

In [RX96] it is shown that on average this algorithm has polylogarithmic run-time complexity. The argument given uses the fact that on uniformly sampled DFAs almost all pairs of states have a shortest distinguishing word of polylogarithmic depth. This fact is attributed to [TB73]. Although this is true for uniformly sampled DFAs, we like to stress that for many use cases and real-life applications this bound does not apply. For example, in the Fibonacci automata presented in Section 5.2 this is not the case. In the automaton *Fib_i* containing *n* states, there is a pair of states for which the shortest distinguishing word, and thus also the number of iterations, has length $n - 2$.

3.4. Partition refinement using partial transitive closure. In this section, we present a new DFA minimisation algorithm `transPR`. The main idea of the algorithm is to perform partition refinement like the algorithms before, but in the initialization compute the transitive

Algorithm 4 Parallel sorting-based algorithm **sortPR****Input:** A DFA $A = (Q, \Sigma, \delta, F, q_0)$, where $|Q| = n$ and $|\Sigma| = k$ **Output:** The minimal quotient automaton represented in the array *block*

```

1: block :: Array[n] of type  $\mathbb{N}$ 
2: state :: Array[n] of type  $Q$ 
3: signature :: Array[n][k] of type  $Q$ 
4: new_block :: Array[n] of type  $\mathbb{N}$ 
5: num_blocks := 2
6: do in parallel for  $q \in Q$ 
7:   block[q] := ( $q \in F$  ? 0 : 1) ▷ Initialize
8:   state[q] := q
9: repeat
10:  num_blocks := new_block[n - 1] + 1 ▷ Number of blocks before iteration
11:  do in parallel for  $q, a \in Q \times \Sigma$ 
12:    signature[q][a] := block[ $\delta(q, a)$ ]
13:  sort(state, COMPARE)
14:  new_block := adjacent_diff(state, ARE_NEQ) ▷ Place 1 for each change
15:  new_block[0] := 0
16:  new_block := inclusive_scan(new_block) ▷ Compute new block labels
17:  do in parallel for  $q \in Q$ 
18:    block[state[q]] = new_block[q]
19: until new_block[n - 1] + 1 = num_blocks

20: function COMPARE( $q_1, q_2$ )
21:  if block[ $q_1$ ] > block[ $q_2$ ] then return false
22:  if block[ $q_1$ ] < block[ $q_2$ ] then return true
23:  for all  $a \in \Sigma$  do
24:    if signature[ $q_1$ ][a] > signature[ $q_2$ ][a] then return false
25:    if signature[ $q_1$ ][a] < signature[ $q_2$ ][a] then return true
26:  return false

27: function ARE_NEQ( $q_1, q_2$ )
28:  if block[ $q_1$ ] ≠ block[ $q_2$ ] then return true
29:  for all  $a \in \Sigma$  do
30:    if signature[ $q_1$ ][a] ≠ signature[ $q_2$ ][a] then return true
31:  return false

```

closure on each distinct letter. After this initialization step, we use **naivePR** to complete the minimisation.

This approach is presented in Algorithm 5. This is done in a data-parallel way which is also used for prefix sum and finding the end of a linked list [HJ86]. On some DFAs, with a rather specific structure, this method exponentially improves the runtime compared to the other partition refinement algorithms.

The algorithm works by adding letters for increasingly large words of the same letters. Given an input DFA $A = (Q, \Sigma, \delta, F, q_0)$, we construct a DFA $A' = (Q, \Sigma^T, \delta^T, F, q_0)$ which

Algorithm 5 Parallel partition refinement with transitive closure **transPR**

-
- 1: $\Sigma^T := \{a^{2^i} \mid a \in \Sigma, i \in [0, \lfloor \log n \rfloor]\}$
 - 2: $\delta^T :: Q \times \Sigma^T \mapsto Q$
 - 3: $\delta^T(q, a) := \delta(q, a)$ for all $a \in \Sigma$
 - 4: **for all** $i \in [1, \lfloor \log n \rfloor]$ **do**
 - 5: **for all** $a \in \Sigma$ **do**
 - 6: **do in parallel for** $q \in Q$
 - 7: $\delta^T(q, a^{2^i}) := \delta^T(\delta^T(q, a^{2^{i-1}}), a^{2^{i-1}})$
 - 8: Perform **naivePR** on the DFA $A' = (Q, \Sigma^T, \delta^T, F, q_0)$
-

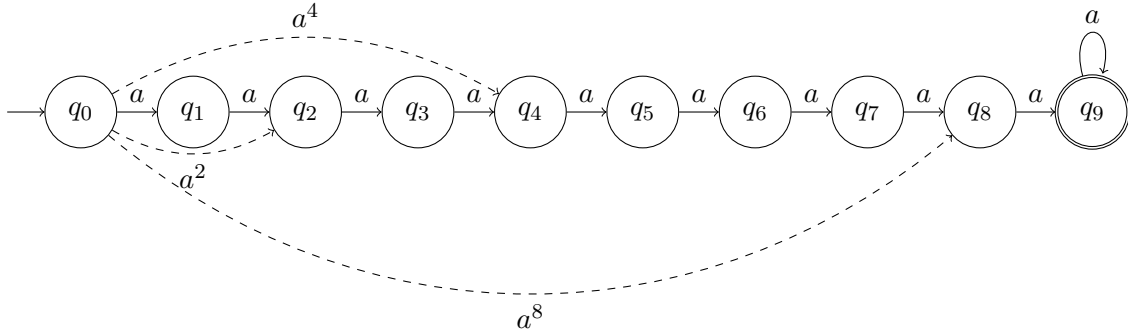


Figure 1: The DFA $A = (\{q_0, \dots, q_9\}, \{a\}, \delta, \{q_9\}, q_0)$ with the extra partial transitive closure from q_0 added in dashed arrows.

has the same set of states and final states, but a larger alphabet Σ^T . The alphabet contains the letters $a^{2^0}, a^{2^1}, \dots, a^{2^{\lfloor \log n \rfloor}}$ for each original letter $a \in \Sigma$. The transition function is computed such that for each new symbol $a^k \in \Sigma^T$ the transition function $\delta^T(q_1, a^k) = q_k$ if in the original DFA Q there are states $q_1, \dots, q_k \in Q$ such that $\delta(q_i, a) = q_{i+1}$ for each $i \in [1, k]$. This can be computed in a logarithmic number of parallel steps, by using the previously computed transitions, as is done at 1.7 of Algorithm 5.

The correctness of this algorithm relies on the fact that equality on states is invariant under the partial closure that is added. Indeed, we can see that the DFA A' obtained in Algorithm 5 is language equivalent to the input DFA A if we consider the alphabet letters added as words. If $\delta^T(q, a_T) = q'$ for some $a_T \in \Sigma^T$, then $a_T = a^{2^j}$ for some $a \in \Sigma$ and $j \in [0, \lfloor \log n \rfloor]$. By construction there is a sequence q_0, \dots, q_k such that $q_0 = q$, $q_{i+1} = \delta(q_i, a)$ and $q_k = q'$.

This approach helps in the case of long paths with the same letter. Consider the DFA A from Figure 1. This DFA accepts all words a^j with $j > 8$. Any parallel partition refinement algorithm would need at least 8 iterations to conclude that q_0 is not the same as q_1 . However, building the partial transitive closure only requires a logarithmic number of parallel iterations. With this partial transitive closure added, a partition refinement algorithm can in the first iteration conclude that q_0 is different from q_1 since the transition with a^8 leads to different states.

4. DFA EQUIVALENCE CHECKING AND INCLUSION CHECKING

So far, we have focussed on DFA minimisation algorithms. Another classical operation on DFAs is *equivalence checking*, which has its practical uses in formal verification, in particular model checking, and compiler construction.

DFA equivalence checking entails checking whether or not two given DFAs have the same language. This can be done via DFA minimisation [Hop71], but it can also be performed with the well-known Hopcroft-Karp algorithm [HK71, AHU74]. Algorithm 6 presents this algorithm. Given two DFAs A and B , a relation R is built, that relates states of A with states of B . In other words, the algorithm tries to build a bisimulation relation between the DFAs. If it succeeds in doing so, the DFAs accept the same language.

At line 1, R is initialised as an empty set, and another set S is created to store the pairs of states that still need to be processed. In the while-loop at lines 2–9, this processing of pairs in S is performed. At line 3, an arbitrary pair $\langle q^A, q^B \rangle$ is selected and removed from S . If the two states q^A and q^B are already related by R^+ , i.e., the transitive closure of R , then no work needs to be done for this pair. Otherwise, it must be checked whether or not exactly one of the two states is accepting (line 5). If that is the case, then A and B do not have the same language, and **false** is returned. Otherwise, for all $a \in \Sigma$, the states $\delta^A(q^A, a)$ and $\delta^B(q^B, a)$ are combined in a new pair and added to S (lines 7–8). By doing so, checks are added that if a particular letter is followed from both q^A and q^B , then the states reached by doing so are again bisimilar. Next, $\langle q^A, q^B \rangle$ is added to R . If all the checks in S succeed, eventually S will be empty, and hence **true** will be returned (line 10).

Algorithm 6 Hopcroft-Karp DFA equivalence checking algorithm

Input: DFAs $A = (Q^A, \Sigma^A, \delta^A, F^A, q_0^A)$ and $B = (Q^B, \Sigma^B, \delta^B, F^B, q_0^B)$
Output: **true** iff $\mathcal{L}(A) = \mathcal{L}(B)$

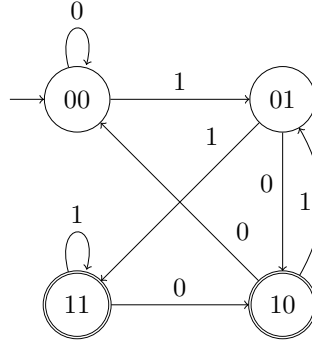
```

1:  $R := \emptyset; S := \{\langle q_0^A, q_0^B \rangle\}$ 
2: while  $S \neq \emptyset$  do
3:   Select  $\langle q^A, q^B \rangle$  from  $S$ ;  $S := S \setminus \{\langle q^A, q^B \rangle\}$ 
4:   if  $\langle q^A, q^B \rangle \notin R^+$  then
5:     if  $(q^A \in F^A \wedge q^B \notin F^B) \vee (q^A \notin F^A \wedge q^B \in F^B)$  then return false
6:     else
7:       for all  $a \in \Sigma$  do
8:          $S := S \cup \{\langle \delta^A(q^A, a), \delta^B(q^B, a) \rangle\}$ 
9:        $R := R \cup \{\langle q^A, q^B \rangle\}$ 
10: return true

```

The check at line 4 requires maintaining the transitive closure of R . Hopcroft and Karp achieve this with a union-find data structure, to keep track of a set of state equivalence classes instead of a set of individual state pairs. As state pairs are added to R at line 9, these equivalence classes are updated. The use of this data structure results in the algorithm having a near-linear complexity.

Maintaining such a union-find data structure in a massively parallel way is highly non-trivial. An alternative is to maintain the set of state pairs that are added to R without updating its transitive closure. While this negatively impacts the algorithm's complexity, this may be mitigated by performing the algorithm massively parallel on a GPU. In practice, sets of elements are typically maintained by means of a hash table. Although not commonly

Figure 2: The DFA memory_2 .

```

1  model memory_2 {
2    actions t, f
3    classes
4    P {
5      variables
6      Boolean b0_0, b1_0, b0_1, b1_1
7      state machines
8      SMO {
9        forbidden Error initial S
10       transitions
11         S -> S { <f> [b1_0 := b0_0; b0_0 := false] }
12         S -> S { <t> [b1_0 := b0_0; b0_0 := true] }
13         S -> Error { (b1_0 and not b1_1) or (not b1_0 and b1_1) }
14       }
15       SM1 {
16         initial S
17         transitions
18         S -> S { <f> [b1_1 := b0_1; b0_1 := false] }
19         S -> S { <t> [b1_1 := b0_1; b0_1 := true] }
20       }
21     }
22     objects p: P()
23 }

```

Figure 3: An SLCO model to check equivalence of two instances of memory_2 .

used, hash tables for GPUs have been developed in recent years [Les19, AAP⁺23, WO23b, HWWL24]. For this article, we use a GPU hash table developed for the explicit-state model checker GPUEXPLORE [WO23b, WO23a, WO24]. This model checker accepts as input models that consist of a finite number of state machines that can synchronise on transition actions and that can read from and write to Integer and Boolean variables. Next, we show how the problem of checking whether two DFAs are equivalent via the ‘naive’ version of the Hopcroft-Karp algorithm, i.e., the version in which a set of state pairs is maintained, can be encoded as an input model for GPUEXPLORE. Given such a model, GPUEXPLORE will construct its state space, which corresponds directly with the construction of the relation R . An on-the-fly check corresponding with line 5 of Algorithm 6 achieves that GPUEXPLORE terminates early and reports a problem whenever the two DFAs are not equivalent.

A variant of the algorithm by Hopcroft and Karp can be used to perform *inclusion checking*, i.e., checking that the language of the first DFA is included in the language of the second DFA. To do this, the condition at line 5 of Algorithm 6 must be changed to $a^A \in F^A \wedge q^B \notin F^B$, other words, the second disjunct of the original condition must be dropped.

An example DFA is given in Figure 2. This DFA is instance 2 of the **memory** benchmark, i.e., **memory**₂ (see Section 5.1). It reads a sequence of bits, and remembers the last two bits it has read. In the initial state, those two bits are initialised to 0.

Figure 3 presents a way to encode equivalence checking of two instances of **memory**₂. This is done using the *Simple Language of Communicating Objects* (SLCO) [Eng12, dPWZ18, Wij23], which is one of the accepted input languages of GPUEXPLORE. A model may have actions (see line 2), in this case **t**, corresponding with 1, and **f**, corresponding with 0. Furthermore, a model can contain a number of *classes*. In this case, there is only the class **P**. A class, in turn, may have a number of variables. For this example, variables are needed to store the two most recent bits, for both instances of **memory**₂, therefore the Boolean variables **b0_0**, **b1_0**, **b0_1** and **b1_1** are declared at line 6. Two state machines, representing the two DFAs, are given at lines 8–14 and lines 15–20.

For the first state machine, **SM0**, an **initial** state **S** and a **forbidden** state **Error** are declared at line 9. Two transitions represent the transitions of the DFA, at lines 11–12. The notation $S \rightarrow S \{ \langle a \rangle [x_0 := E_0; x_1; E_1] \}$ should be interpreted as follows. If the state machine is in state **S**, then it can transition to state **S** if action **a** can be fired, and when this occurs, the assignments $x_0 := E_0$ and $x_1 := E_1$ will be executed in order, in one atomic step.

Note at line 13 the transition to the **forbidden** state **Error**. This transition is enabled iff the expression associated with it, between the curly brackets, evaluates to **true**. Note furthermore that this condition corresponds with the condition at line 5 of Algorithm 6. Whenever the **Error** state is reached when performing state space exploration, GPUEXPLORE will terminate and report the error, which in this case represents the in-equivalence of the two DFAs.

State machine **SM1** is almost a copy of **SM0**, apart from the use of an **Error** state. Since **SM1** has the same actions **t** and **f** associated with transitions, and therefore in its alphabet, **t** and **f** need to synchronise: a **t**-transition (**f**-transition) of **SM0** can be followed iff a **t**-transition (**f**-transition) of **SM1** can be followed, and when this is done, the two state machines transition together in one step. This mechanism achieves that exploration of the state space of model **memory**₂ corresponds with constructing the synchronous product of **SM0** and **SM1**, and therefore of the two DFAs.

Finally, at line 22, an instance of class **P**, the **object** **p**, is created. In SLCO, classes can be instantiated multiple times, but in this application, only a single class instance is necessary.

Note in the example that the DFAs, as described in an SLCO model, are not explicitly given, but instead described at a higher level, i.e., specified. In this particular example, for instance, the four states of DFA **memory**₂ are not explicitly represented by four states of an SLCO state machine, and its eight transitions are also not represented by eight SLCO transitions directly, but instead captured by the two transitions at lines 11–12 (and 18–19) of Figure 3. While this means that in our approach, state space exploration does not only entail computation of the synchronous product, but also the construction of the actual input DFAs, we argue that this is not only practically necessary, but also realistic. An explicit encoding of

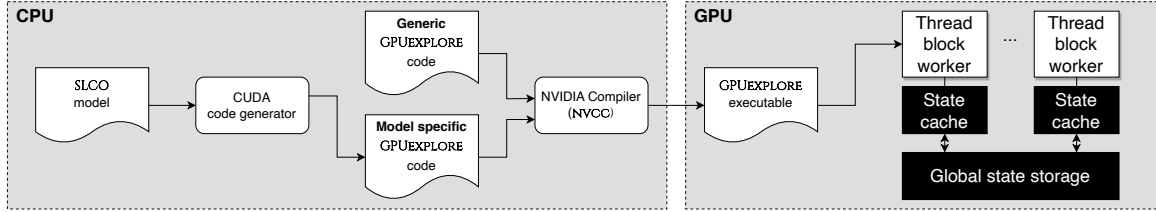


Figure 4: The workflow from SLCO model to GPUEXPLORE model checking.

a DFA in SLCO is feasible, but as the DFAs become larger, such an encoding would quickly become unwieldy, and GPUEXPLORE would not be able to process the resulting models. In practice, however, for the vast majority of DFAs, a high-level description is available from which a specification can be derived as we have in our example SLCO model. In other words, typically, a DFA is not a randomly constructed automaton, but instead there is some rational behind its creation, which can be used to construct a specification.

To perform inclusion checking with GPUEXPLORE, the condition to transition to the **Error** state must be changed in the same way as the condition at line 5 of Algorithm 6. For instance, at line 13 of Figure 3, the transition should be changed to `S -> Error { b1_0 and not b1_1 }`.

GPUEXPLORE. Figure 4 presents the workflow from SLCO model to model checking with GPUEXPLORE. Given an SLCO model, a code generator, written in PYTHON, generates CUDA C++ code to interpret the model: for every transition in the model, code is generated to check whether the transition can be fired, and to actually fire the transition. This code is combined with generic code, i.e., code not specific for a particular SLCO model. This code contains, for instance, an implementation of the used GPU hash table. Next, NVIDIA’s NVCC compiler compiles the combined code, resulting in an executable that can be launched on an NVIDIA GPU. In practice, it has been shown that GPU-acceleration of explicit-state model checking can be very efficient, with speedups of hundreds of times compared to state-of-the-art CPU-based explicit-state model checkers [WO23a, WO24, OW24].

On the right in Figure 4, an overview is given of how GPUEXPLORE runs on a GPU. A global hash table, containing the constructed states, resides in global memory. Many thread blocks, each containing 512 threads, scan this hash table for states that require exploration, i.e., for which their outgoing transitions need to be checked and potential successor states need to be constructed. States that require exploration are temporarily stored in *shared memory*, which is fast, but small, on-chip memory that the threads in a block can use together. Any constructed successor states are stored in a shared memory hash table, before they are synchronised with the global memory hash table. This process is massively parallel, with the threads in each block working together on both successor generation and global memory storage. This is repeated until all the states reachable from the initial state have been identified. More information on GPUEXPLORE can be found in [WB14, WNB16, WB16, WO23a, WO23b, OW24, WO24].

5. EXPERIMENTS

In this section, we discuss the results of our implementations. We benchmarked the implementations of DFA minimisation algorithms with respect to three families of DFAs: Fibonacci

DFAs Fib_k from [CRS08], bit-splitters \mathcal{B}_k derived from [GMdV23], and DFAs derived from a subset of the VLTS benchmark set.² Our approach to DFA equivalence checking has been benchmarked using two families of DFAs: one inspired by the Fibonacci DFAs that are cyclic, similar to the Fibonacci DFAs, but contrary to the latter, can have more than one letter and do not involve Fibonacci words over the binary alphabet. We call these DFAs *Cycle DFAs* \mathcal{C}_k , and a family \mathcal{B}'_k that extends the bit-splitters with an initial state, as the original bit-splitters do not have one.

5.1. Benchmarks.

Fibonacci DFAs: The first family of DFAs we use for benchmarking consists of so-called Fibonacci automata. These are simple automata with only a unary alphabet. However, they exhibit very particular behaviour. As witnessed in [CRS08], these automata are notoriously hard for partition refinement and the number of iterations of any partition refinement algorithm is n . The automata are called Fibonacci automata due to the close correspondence with Fibonacci words over the binary alphabet, which are defined inductively as follows: the base cases are $w_0 = 1$, and $w_1 = 0$, and for every $i \in \mathbb{N}$, $w_{n+1} = w_n w_{n-1}$. This gives the following sequence:

$$\begin{aligned} w_2 &= 01 \\ w_3 &= 010 \\ w_4 &= 01001 \\ w_5 &= 01001010 \\ &\dots \end{aligned}$$

For every $n \in \mathbb{N}$, we define the automaton $\text{Fib}_n = (Q, \{a\}, \delta, q_0, F)$ as follows, with $w_n[i]$ referring to the i -th bit in the bit sequence w_n :

- the set of states is $Q = \{q_i \mid i \in [0, |w_n|]\}$;
- the transition function is $\delta(q_i, a) = q_{i+1 \bmod |w_n|}$;
- the set of final states is $F = \{q_i \mid q_i \in Q \text{ and } w_n[i] = 1\}$.

The Fibonacci DFA Fib_5 is given in Figure 5.

Bit-splitters: The second family of automata consists of the so-called *bit-splitters* \mathcal{B}_n . For $n \in \mathbb{N}$, the bit-splitter \mathcal{B}_n is a deterministic automaton with 2^n states and an alphabet consisting of $n-1$ symbols. By construction, during partition refinement, every time a block can be split, it is split in two blocks of equal size. This property makes the family inherently hard for partition refinement algorithms. However, the parallel algorithm requires only a logarithmic number of iterations to compute the minimal DFA. The bit splitter \mathcal{B}_3 is given in Figure 5.

The family does not contain an initial state, and comes from the setting of Labelled Transition Systems (LTSs). An LTS is a graph structure with a finite number of states and transitions between states, with each transition having an action label.

Since it is a hard example for partition refinement, we use it for this purpose and allow the absence of an initial state. In the following, states σ represent bit sequences of length n , i.e., $\sigma \in \{0, 1\}^n$. We define $\mathcal{B}_1 = (Q_1, \Sigma_1, \delta_1, F_1)$, where $Q_1 = \{0, 1\}$, $\Sigma_1 = \emptyset$

²<https://cadp.inria.fr/resources/vlts> (visited on: 04-2024).

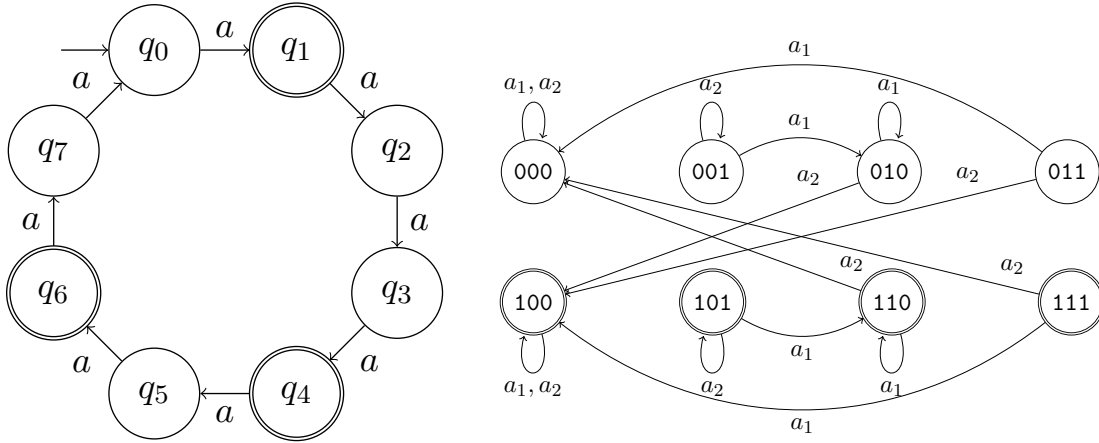


Figure 5: The DFA Fib_5 on the left, and the DFA \mathcal{B}_3 on the right.

and $F_1 = \{1\}$. Given the automaton $\mathcal{B}_n = (Q_n, \Sigma_n, \delta_n, F_n)$ for some $n \in \mathbb{N}$, we define $\mathcal{B}_{n+1} = (Q_{n+1}, \Sigma_{n+1}, \delta_{n+1}, F_{n+1})$, such that:

- The set of states contains two copies of Q_n , i.e., $Q_{n+1} = \{0\sigma, 1\sigma \mid \sigma \in Q_n\}$,
- One fresh symbol $a_n \notin \Sigma_n$ is added to the alphabet: $\Sigma_{n+1} = \Sigma_n \cup \{a_n\}$,
- The transition function δ_{n+1} is defined such that for each $a_m \in \Sigma_n$, and state $\mathbf{b}\sigma \in Q_{n+1}$, it maintains the behaviour of \mathcal{B}_n , i.e., $\delta_{n+1}(\mathbf{b}\sigma, a_m) = \mathbf{b}\delta_n(\sigma, a_m)$. For the fresh symbol $a_n \in \Sigma_{n+1} \setminus \Sigma_n$, δ_{n+1} is extended as follows, with $\bar{\mathbf{b}}$ being the bit flipped version of \mathbf{b} , i.e., $\mathbf{b} = 0 \iff \bar{\mathbf{b}} = 1$:

$$\delta_{n+1}(\mathbf{b}\sigma, a_n) = \begin{cases} \bar{\mathbf{b}}\sigma & \text{If } \sigma[0] = 1, \\ \mathbf{b}\sigma & \text{otherwise.} \end{cases}$$

- the set of accepting states is $F_{n+1} = \{1\sigma \mid \sigma \in Q_n\}$.

As previously mentioned, bit-splitter DFAs are constructed in such a way that they are inherently hard to minimize by partition refinement. Each bit-splitter \mathcal{B}_{n+1} combines two copies of the bit-splitter \mathcal{B}_n , with the transition function defined in such a way that each possible split divides an existing block in two blocks of the same size. This results in a DFA in which the amount of required work for splitting is large, since each split involves moving many states to the new block. However, because in each split a block is split in two parts of the same size, the number of sequential splits needed is smaller than for the Fibonacci automata.

VLTSs: For the benchmarking of our DFA minimisation implementations, we also use the VLTS benchmark suite. The VLTS acronym stands for *Very Large Transition Systems*. This suite consists of LTSs that originate from modelling protocols and concurrent systems. Some of the benchmarks are from case studies from industrial systems.

The transition relation of an LTS does not need to be deterministic, nor complete. We turn an LTS into a DFA by first making the LTS deterministic such that each state has at most one outgoing transition for every label, using the powerset construction algorithm [RS59]. To convert the deterministic LTS to a DFA, we need to complete the transition function and define which states are accepting. We define all the states as accepting and add one new non-accepting state \perp . For each state q and label a for which there exists no transition with that label from q , we add a new transition labelled a to \perp , i.e. $\delta(q, a) = \perp$. This completes

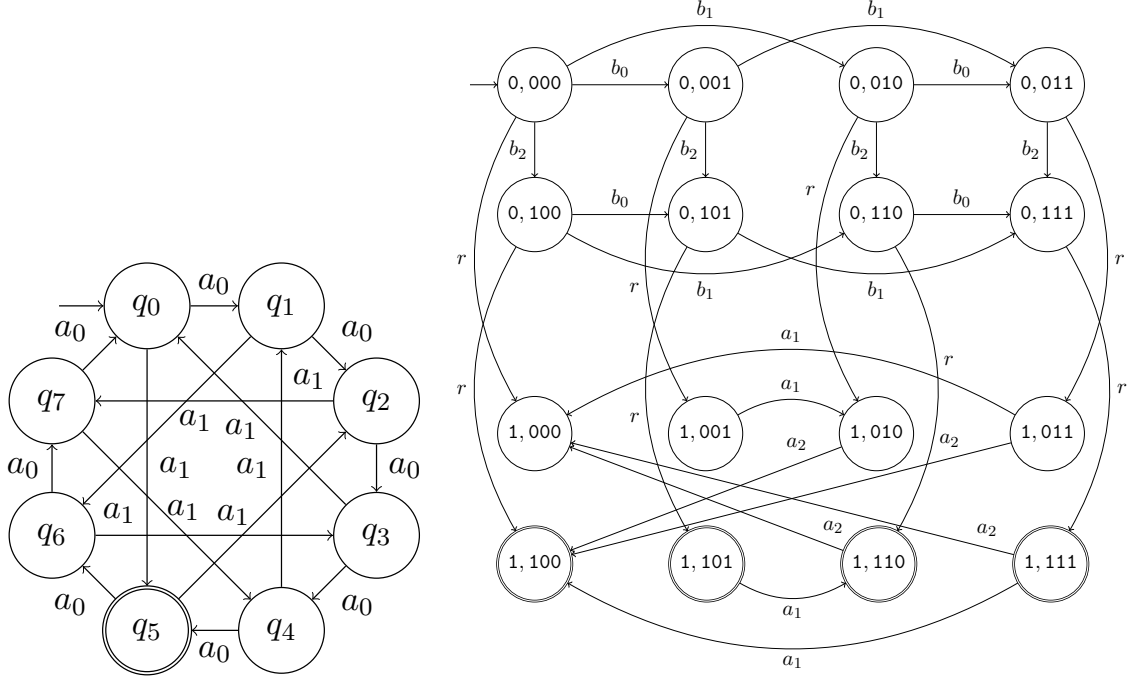


Figure 6: The DFA \mathcal{C}_5 on the left, and the DFA \mathcal{B}'_3 (without self-loops) on the right.

the transition function and creates a DFA accepting all the words corresponding with a path through the original LTS.

Due to state-space explosion we were not able to make all VLTS benchmarks deterministic. We used all benchmarks for which the computation to make them deterministic took less than ten minutes.

Cycle DFAs: This family has been used to benchmark our approach to DFA equivalence checking using the GPU-accelerated model checker GPUEXPLORE. It is inspired by the Fibonacci DFAs, but it differs in two aspects. First of all, the DFAs may involve multiple letters, to make equivalence checking more interesting. Second of all, the correspondence with Fibonacci words over the binary alphabet has been removed, as it cannot be encoded in the input language of GPUEXPLORE, SLCO.

For every $n \in \mathbb{N}$ with $n > 1$, we define the automaton $\mathcal{C}_n = (Q, \Sigma, \delta, q_0, F)$ as follows, with $fib(n)$ referring to the n^{th} Fibonacci number:

- the set of states is $Q = \{q_i \mid i \in [0, fib(n) - 1]\}$;
- the set of actions Σ consists of actions a_0, \dots, a_m , with $m = \max(\lfloor \log_{10}(fib(n)) \rfloor, 1)$, i.e., the rounded logarithm of $fib(n)$ or 1, if that number is 0.
- the transition function is defined as follows, for $j \in [0, m]$:

$$\delta(q_i, a_j) = q_{i+(j \cdot 100)+1} \mod fib(n)$$

- the set of final states is $F = \{q_{fib(n-1)}\}$.

The Cycle DFA \mathcal{C}_5 is given in Figure 6.

Extended bit-splitters: As GPUEXPLORE requires that input automata have an initial state, the bit-splitters can only be used by our approach to DFA equivalence checking if they are extended with an initial state. To achieve this, we extend the states in the bit-splitters to tuples (c, σ) , with the first element being a bit c , and the second being the bit-sequences σ of the original bit-splitters. This effectively doubles the number of states of an extended bit-splitter B'_k compared to B_k .

We define $B'_1 = (Q'_1, \Sigma'_1, \delta'_1, (0, 0), F'_1)$, where $Q'_1 = \{(0, 0), (0, 1), (1, 0), (1, 1)\}$ and $\Sigma'_1 = \{b_0, r\}$. The letter b_0 occurs on transitions in which the second state bit is flipped from 0 to 1, in case the first bit is 0:

$$\delta'_1((c, b), b_0) = \begin{cases} (c, 1) & \text{If } c = 0, \\ (c, b) & \text{otherwise.} \end{cases}$$

The letter r occurs on transitions that set the first bit to 1:

$$\delta'_1((c, b), r) = (1, b)$$

Finally, $F'_1 = \{(1, 1)\}$.

Given the automaton $B'_n = (Q'_n, \Sigma'_n, \delta'_n, F'_n)$ for some $n \in \mathbb{N}$, we define $B'_{n+1} = (Q'_{n+1}, \Sigma'_{n+1}, \delta'_{n+1}, F'_{n+1})$, such that:

- The set of states contains two copies of the σ parts of the states in Q'_n , extended with one bit, combined with the two possible values of c , i.e., $Q'_{n+1} = \{(c, 0\sigma), (c, 1\sigma) \mid c \in [0, 1] \wedge \sigma \in Q'_n\}$,
- Two fresh symbols $a_n, b_{n+1} \notin \Sigma'_n$ are added to the alphabet: $\Sigma'_{n+1} = \Sigma'_n \cup \{a_n, b_{n+1}\}$,
- The transition function δ'_{n+1} is defined such that for each $a_k, b_m \in \Sigma'_n$, and states $(c, b\sigma) \in Q'_{n+1}$, it maintains the behaviour of B'_n , i.e., $\delta'_{n+1}((c, b\sigma), a_k) = (c, b\delta'_n((c, \sigma), a_k))$ and $\delta'_{n+1}((c, b\sigma), b_m) = (c, b\delta'_n((c, \sigma), b_m))$. For the fresh symbols $a_n, b_{n+1} \in \Sigma'_{n+1} \setminus \Sigma'_n$, δ'_{n+1} is extended as follows, with \bar{b} being the bit flipped version of b , i.e., $b = 0 \iff \bar{b} = 1$:

$$\delta'_{n+1}((c, b\sigma), a_n) = \begin{cases} (c, \bar{b}0^n) & \text{If } c = 1 \wedge \sigma[0] = 1, \\ (c, b\sigma) & \text{otherwise.} \end{cases}$$

$$\delta'_{n+1}((c, b\sigma), b_{n+1}) = \begin{cases} (c, \bar{b}\sigma) & \text{If } c = 0 \wedge b = 0, \\ (c, b\sigma) & \text{otherwise.} \end{cases}$$

Finally, δ_{n+1} is extended with r -transitions in the following way:

$$\delta'_{n+1}((c, b\sigma), r) = (1, b\sigma)$$

- the set of accepting states is $F'_{n+1} = \{(1, 1\sigma) \mid \sigma \in Q'_n\}$.

In the extended bit-splitter family of DFAs, the b_i -transitions serve the purpose of manipulating the bits of the initial bit-sequence consisting of all 0's, prior to entering the original bit-splitter DFA, now represented by states in which $c = 1$, and the a_i -transitions between them. The r -transitions indicate moving from the 'initialisation' part of the DFA to the bit-splitter part of the DFA. The extended bit-splitter B'_3 is given in Figure 6, where, for readability, the self-loops are not shown.

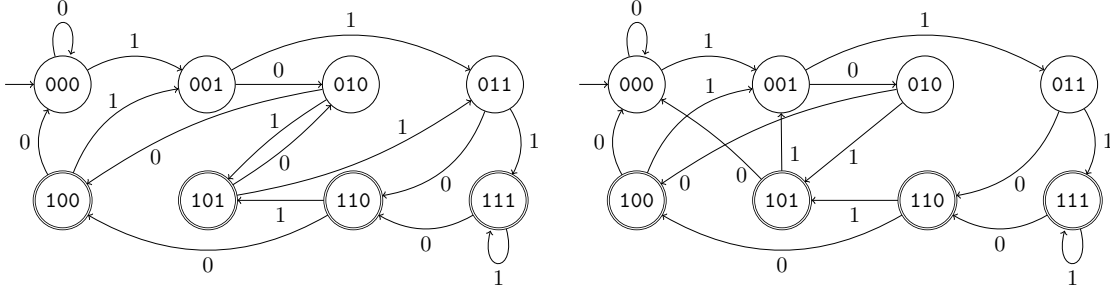


Figure 7: The perfect (left) and forgetful (right) **memory** DFAs for depth $n = 3$.

Memory. The **memory** DFA family is used to perform inclusion checking. For each depth $n \in \mathbb{N}$ two members of this family are defined, referred to as *perfect* and *forgetful*. For both of these, each state of the DFA for depth n encodes information about the last n symbols the DFA has read. The alphabet we use only contains two elements, so each state represents a unique bitstring of length n . For each symbol in the alphabet an outgoing transition with that symbol as the action is defined to the state representing the bitstring of the source state with the respective bit prepended. The most significant bit is discarded. In the forgetful memory DFA all bits are reset after the most significant bits read 10. The *perfect* memory DFA for depth $n = 2$ can be seen in Figure 2, as it is used to explain the encoding of DFA equivalence checking in SLCO models. The *perfect* and *forgetful* memory DFAs for depth $n = 3$ are displayed in Figure 7.

5.2. Results for DFA minimisation. The DFA minimisation algorithms were implemented in CUDA C++ and compiled using the CUDA toolkit 12.2, with the implementation of **sortPR** using the Thrust library for sorting and computing the adjacent differences and inclusive scans [BH12]. Experiments were conducted on a device running Linux Mint 20, equipped with an NVIDIA TITAN RTX GPU with 24 GB of memory and 4,608 cores. Such a GPU can manage trillions of light-weight threads. Thanks to fast context switching between threads, a GPU can typically handle a few hundred thousand threads as if they execute in parallel.

The reported times are the average of five separate runs. Benchmarks that did not finish within five minutes were aborted, in which case we registered a timeout ‘t/o’. Benchmarks for which there was not enough memory are indicated by ‘OoM’.

Transitive approach: The results of running Algorithm 1 on the Fibonacci automata are given in Table 1. As expected, the number of threads used to compute the transitive closure in parallel grows very quickly. Although the number of iterations of the algorithm is indeed logarithmic, the available parallelism is not sufficient to lead to logarithmic run times. We only use this set of small Fibonacci automata for this algorithm. It already suggests that for a relatively small amount of states (~ 100), obtaining the required resources is already infeasible. The other benchmarks are almost completely out of range of the algorithm.

Partition refinement algorithms: The results of running the parallel partition refinement algorithms, **naivePR** (Algorithm 2), **sortPR** (Algorithm 4), and **transPR** (Algorithm 5) are given in Table 2 and Table 3 for the different benchmarks.

First, we observe in Table 2 that on the Fibonacci automata the **naivePR** performs better than **sortPR**. This can be explained by the fact that the number of iterations is n for both

Name	N	Iterations	Time (ms)	Memory(Mb)	#threads
Fib ₄	8	3	0.3	0	589,824
Fib ₅	13	4	0.7	0	6,230,016
Fib ₆	21	5	7.8	0	88,510,464
Fib ₇	34	5	159.9	0	1,620,545,536
Fib ₈	55	6	3,034.9	10	27,955,840,000
Fib ₉	89	7	66,846.7	60	498,865,340,416
Fib ₁₀	144	t/o	t/o	412	8,943,640,510,464

Table 1: Results of running the algorithm **trans** on the Fibonacci automata.

algorithms, while each iteration in **sortPR** is slower than in **naivePR**. Another interesting observation here is that for all benchmarks **Fib**₁₈, . . . , **Fib**₂₈ the run time of the algorithm **naivePR** scales linearly with the number of states n . Since the number of parallel iterations is $n-2$ for all these benchmarks, each parallel iteration processing up to $\sim 500k$ states took a similar amount of time. In other words, the GPU was able to run around $500k$ threads as if they ran in parallel. This confirms the statement about fast context switching at the beginning of Section 5.2.

Finally, for the Fibonacci automata, we see that **transPR** performs significantly better on this benchmark. This can be explained by the fact that the partial transitive closure reduces the number of iterations of the algorithm significantly.

The results on the bit-splitter automata in Table 2 show that the improvement of **transPR** does not work on all automata. The high number of alphabet letters together with the structure of the automata make the transitive closure less effective, making **naivePR** much faster.

For the VLTS benchmark set we see the power of **sortPR** in Table 3. In some benchmarks, like ‘vasy_69_520’ the algorithm performs significantly better. In these examples, it helps that in **sortPR**, in each iteration a block can be split into many subblocks, which is not the case in the other algorithms.

Since the VLTS benchmarks originate from communication protocols and concurrent systems, the success of **sortPR** suggests that for DFAs that represent ‘real’ systems, this algorithm is a solid choice for efficient DFA minimisation. However, the experiments with the Fibonacci and bit-splitter families of DFAs demonstrate room for improvement.

5.3. Results for DFA equivalence and inclusion checking. As explained in Section 4, high-level descriptions of the two DFAs involved in equivalence or inclusion checking are written in the SLCO model checking language before the state space of their synchronous product is explored using the GPUEXPLORE model checking tool. Depending on the model checking task, GPUEXPLORE reports multiple timing metrics related to the running time of the state space exploration task. Each time such a task is initiated, a CUDA context needs to be initialised, which takes up to a second. We refer to the time this takes as the *initialisation time*. The time spent on actually exploring the state space is called the *exploration time*, which is measured separately. In theory it should be possible to eliminate most of the initialisation time when running multiple exploration tasks by using the same CUDA context, but we have not implemented this functionality.

We have tested the benchmarks on two different systems. One system has an Intel i5TM 6600k processor with 32GB of DDR4 RAM. The system is equipped with two NVIDIA

Name	Benchmark metrics			Times (ms)			Iterations		
	N	$ \Sigma $	Size output	naivePR	sortPR	transPR	naivePR	sortPR	transPR
Fib ₁₈	6,765	1	6,765	118.6	979.0	1.0	6,764	6,764	5
Fib ₁₉	10,946	1	10,946	191.7	2,085.9	1.1	10,945	10,945	12
Fib ₂₀	17,711	1	17,711	308.8	3,909.2	1.7	17,710	17,710	14
Fib ₂₁	28,657	1	28,657	494.2	6,374.2	2.4	28,656	28,656	25
Fib ₂₂	46,368	1	46,368	778.7	11,712.1	4.1	46,367	46,367	61
Fib ₂₃	75,025	1	75,025	1,241.3	21,366.6	8.0	75,024	75,024	101
Fib ₂₄	121,393	1	121,393	2,006.7	34,793.1	12.5	121,392	121,392	104
Fib ₂₅	196,418	1	196,418	3,251.3	64,411.7	18.3	196,417	196,417	138
Fib ₂₆	317,811	1	317,811	5,277.8	178,367.4	49.8	317,810	317,810	102
Fib ₂₇	514,229	1	514,229	8,607.7	t/o	96.1	514,228	t/o	268
Fib ₂₈	832,040	1	832,040	22,723.0	t/o	178.4	832,039	t/o	299
Fib ₂₉	1,346,269	1	1,346,269	59,510.8	t/o	726.9	1,346,268	t/o	755
Fib ₃₀	2,178,309	1	2,178,309	141,601.0	t/o	1,109.3	2,178,308	t/o	914
B ₁₅	32,768	14	32,768	0.8	25.8	1.7	14	14	2
B ₁₆	65,536	15	65,536	1.4	29.7	3.7	15	15	2
B ₁₇	131,072	16	131,072	2.6	54.3	9.4	16	16	2
B ₁₈	262,144	17	262,144	5.0	107.2	25.6	17	17	2
B ₁₉	524,288	18	524,288	9.6	235.7	60.9	18	18	2
B ₂₀	1,048,576	19	1,048,576	19.3	520.2	139.8	19	19	2
B ₂₁	2,097,152	20	2,097,152	39.8	1,148.6	312.2	20	20	2
B ₂₂	4,194,304	21	4,194,304	82.6	2,538.5	728.7	21	21	2
B ₂₃	8,388,608	22	8,388,608	170.3	5,612.7	1,612.1	22	22	2
B ₂₄	16,777,216	23	16,777,216	352.6	12,351.8	OoM	23	23	OoM
B ₂₅	33,554,432	24	33,554,432	737.4	27,092.2	OoM	24	24	OoM
B ₂₆	67,108,864	25	67,108,864	1,541.5	59,203.8	OoM	25	25	OoM

Table 2: Results of running the partition refinement algorithms on the **Fib** and **B** benchmark set.

Titan RTX graphics cards, each containing 4,608 CUDA cores and 24GB of GDDR6 VRAM running with a memory clock of 1,750 MHz, at a 384-bit bus width. We only use one card at a time for these benchmarks.

The other system has an AMD Ryzen™ 7 5800X, installed on an MSI MPG x570 Gaming Pro Carbon Wi-Fi motherboard, with 32GB of DDR4 RAM. This system is equipped with an NVIDIA RTX 3090 GPU, with 10,496 CUDA cores and 24GB of GDDR6X VRAM running with a memory clock of 1,219 MHz, at a 384-bit bus width.

The state count of each state space along with all results are displayed in Table 4. For all models in this table, the equivalence checking is trivial, i.e. we compare a DFA with itself. This means that the size of the resulting product is equivalent to the size of the input DFA, which means that worst-case, the running time is linear. While there are some irregularities for lower state counts, the graphs for extended bit-splitter and Cycle DFAs support this proposition.

The results for the extended bit-splitter experiments are presented in Figure 8. In the lower range, the exploration time of equivalence checking of extended bit-splitter DFAs follows a peculiar trajectory that we have found difficult to explain. Up to $n = 13$ the exploration time increases very sharply, but from $n = 13$ to $n = 14$ the exploration time actually decreases. This pattern occurs for both the Titan RTX and the RTX 3090 systems. We believe this is related to the data type used for describing the individual states in the synchronous product, i.e., the elements stored in the global hash table. For n up to 13,

Name	Benchmark metrics			Times (ms)			Iterations		
	N	$ \Sigma $	Size output	naivePR	sortPR	transPR	naivePR	sortPR	transPR
cwi_1_2	4,448	26	2,416	5.4	66.7	25.1	308	38	621
cwi_2416_17605	503	15	58	0.8	38.2	0.4	40	40	8
cwi_3_14	63	2	63	1.2	9.1	0.4	61	61	8
vasy_0_1	92	2	10	0.2	3.9	0.4	6	5	5
vasy_1_4	6,087	6	29	0.4	8.5	0.9	15	7	20
vasy_10_56	10,850	12	2113	8.7	40.2	30.9	519	33	791
vasy_1112_5290	1,112,491	23	266	135.4	386.8	2,049.2	246	4	231
vasy_157_297	157,605	235	4,290	455.1	1,736.3	11,312.0	1,049	27	1,306
vasy_164_1619	109,911	37	1,025	69.9	50.5	823.4	770	4	766
vasy_166_651	393,147	211	392,175	159,265.6	1,070.6	t/o	175,764	19	t/o
vasy_18_73	419,664	17	31,952	1,586.1	305.2	34,055.2	13,343	27	18,444
vasy_25_25	25,218	25,216	25,218	262,878.6	3,502.7	t/o	25,217	2	t/o
vasy_386_1171	355,790	73	114	36.9	489.4	766.0	58	8	113
vasy_40_60	40,007	3	40,007	331.6	8,391.5	845.2	20,004	20,002	20,004
vasy_5_9	5,088	31	138	2.2	14.3	7.0	113	5	124
vasy_574_13561	574,058	141	3,578	2,332.2	976.5	64,312.6	2,351	5	2,634
vasy_6120_11031	3,190,785	125	5,216	13,186.6	21,886.0	t/o	2,373	21	t/o
vasy_65_2621	65,538	72	65,537	2,591.8	38.3	47,568.0	36,575	4	38,999
vasy_66_1302	209,791	81	208,419	42,864.9	96.0	t/o	179,861	8	t/o
vasy_69_520	74,958	135	74,958	7,223.0	124.2	181,611.4	49,723	12	74,667
vasy_720_390	87,741	49	3,279	176.0	57.1	2,961.7	2,936	5	2,950
vasy_8_24	20,306	11	560	5.9	26.8	22.1	282	17	348
vasy_8_38	8,922	81	220	5.7	44.1	31.5	174	5	215
vasy_83_325	393,147	211	392,175	162,495.0	1,074.4	t/o	173,218	19	t/o

Table 3: Results of running the partition refinement algorithms on the VLTS benchmark set.

a 32-bit integer suffices to represent a state, but starting with $n = 14$, a 64-bit integer is required for this. While one might expect the performance to suffer from the size increase, we hypothesise that better chunk alignment can actually increase the performance of memory accesses when using larger datatypes, and since a size of 64 bits is still well within the bus width of the GPUs, it is to be expected that the increased size does not decrease performance of any other operations.

The results for the Cycle DFA experiments are shown in Figure 9. Where the RTX 3090 clearly outperformed the Titan RTX for the bit-splitter experiments, for the Cycle DFAs we can see that their times are a lot closer. For some models, the Titan RTX even beats the RTX 3090. While most hardware specifications are higher for the RTX 3090, the memory clock speed of the Titan RTX is higher than that of the RTX 3090. We suspect the performance of equivalence checking of Cycle DFAs may be bottlenecked by the memory throughput and frequency.

We used the perfect and forgetful `memory` models to perform inclusion checking. Since the models we compare are not equivalent, the resulting product can grow larger than the input DFAs, up to quadratic size. When exploring the state space of the `memory` model instances, the increase in states over the base DFAs was noticeable but not dramatic.

The benchmark checks if the language of the forgetful `memory` model is included in the language of the perfect `memory` model. This inclusion is valid, as forgetting the state and resetting to the initial state only rejects a set of otherwise accepting inputs, and does not lead to accepting inputs that would otherwise have been rejected. The results for this are shown in Table 5, and a graph of the metrics is provided in Figure 10. The exploration times for the `memory` model instances are typically very low, so it is hard to draw conclusions about

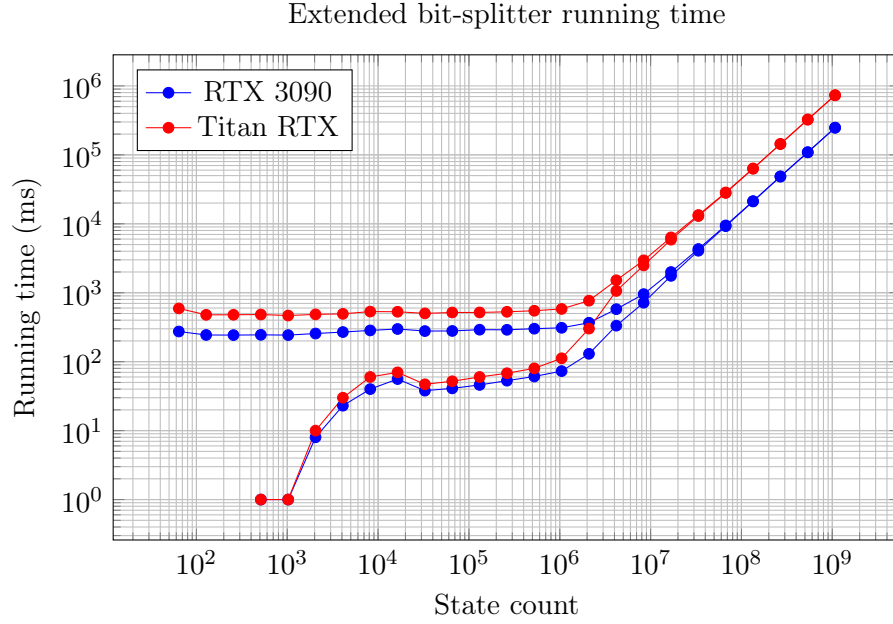


Figure 8: Exploration time and total time for different configurations of extended bit-splitter, ranging from $n=5$ up to and including $n=29$. The total time includes the initialization time of the CUDA context.

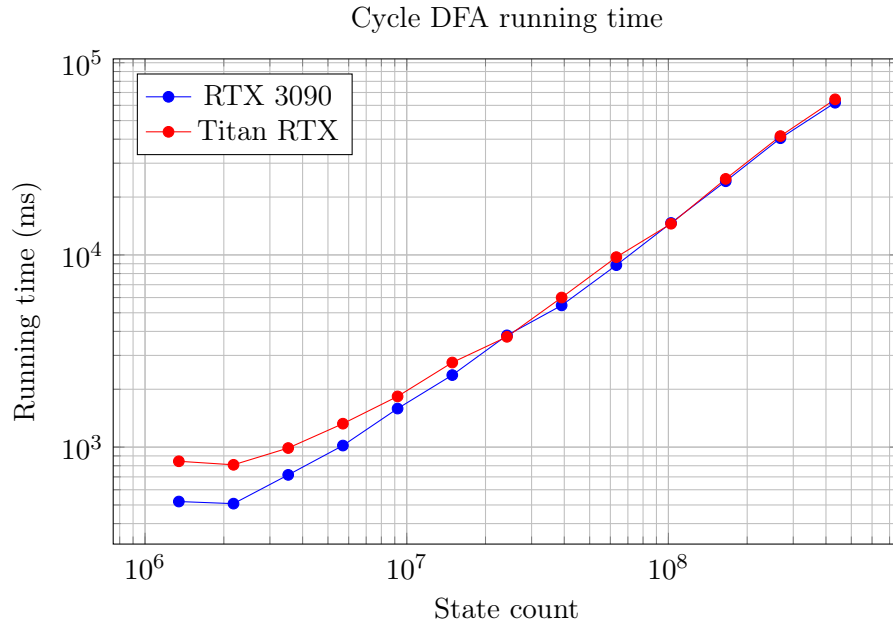


Figure 9: Total time for different configurations of Cycle DFA, ranging from $n=30$ up to and including $n=43$. The running time is not shown separately because it did not differ significantly from the total runtime, and it made the graph too cluttered.

Name	Benchmark metrics	RTX 3090 Times (ms)			Titan RTX Times (ms)		
	State count	Total	Initial	Exploration	Total	Initial	Exploration
B ₅ '	64	274	274	0	592	591	0
B ₆ '	128	244	244	0	478	477	0
B ₇ '	256	243	243	0	479	478	0
B ₈ '	512	245	244	1	483	482	1
B ₉ '	1,024	243	243	1	467	466	1
B ₁₀ '	2,048	256	248	8	485	475	10
B ₁₁ '	4,096	269	246	23	494	464	30
B ₁₂ '	8,192	284	244	40	533	472	60
B ₁₃ '	16,384	298	242	56	530	460	70
B ₁₄ '	32,768	278	240	38	502	456	47
B ₁₅ '	65,536	279	238	41	517	465	52
B ₁₆ '	131,072	291	245	46	518	458	60
B ₁₇ '	262,144	290	237	53	529	460	68
B ₁₈ '	524,288	301	240	61	548	469	80
B ₁₉ '	1,048,576	310	237	73	582	470	112
B ₂₀ '	2,097,152	367	237	130	767	465	302
B ₂₁ '	4,194,304	578	245	333	1,517	453	1,063
B ₂₂ '	8,388,608	955	239	717	2,951	460	2,491
B ₂₃ '	16,777,216	1,997	240	1,757	6,347	460	5,887
B ₂₄ '	33,554,432	4,308	243	4,065	13,403	456	12,947
B ₂₅ '	67,108,864	9,467	240	9,227	28,490	451	28,039
B ₂₆ '	134,217,728	21,326	243	21,083	63,432	480	62,951
B ₂₇ '	268,435,456	48,648	242	48,407	143,937	459	143,478
B ₂₈ '	536,870,912	109,184	247	108,936	325,268	466	324,802
B ₂₉ '	1,073,741,824	247,849	241	247,607	732,229	464	731,764
C ₃₀	1,346,269	521	282	239	844	572	271
C ₃₁	2,178,309	508	158	350	809	438	371
C ₃₂	3,524,578	717	161	556	989	436	553
C ₃₃	5,702,887	1,019	162	857	1,324	441	883
C ₃₄	9,227,465	1,587	157	1,430	1,836	442	1,394
C ₃₅	14,930,352	2,370	157	2,212	2,755	430	2,324
C ₃₆	24,157,817	3,815	159	3,655	3,749	441	3,307
C ₃₇	39,088,169	5,463	165	5,297	6,002	436	5,564
C ₃₈	63,245,986	8,845	167	8,676	9,739	429	9,308
C ₃₉	102,334,155	14,665	160	14,502	14,530	441	14,085
C ₄₀	165,580,141	24,170	160	24,005	24,866	437	24,424
C ₄₁	267,914,296	40,477	157	40,313	41,525	445	41,071
C ₄₂	433,494,437	61,922	160	61,752	64,497	435	64,049

Table 4: Results of running GPUEXPLORE on the extended bit-splitter and Cycle DFA benchmark sets.

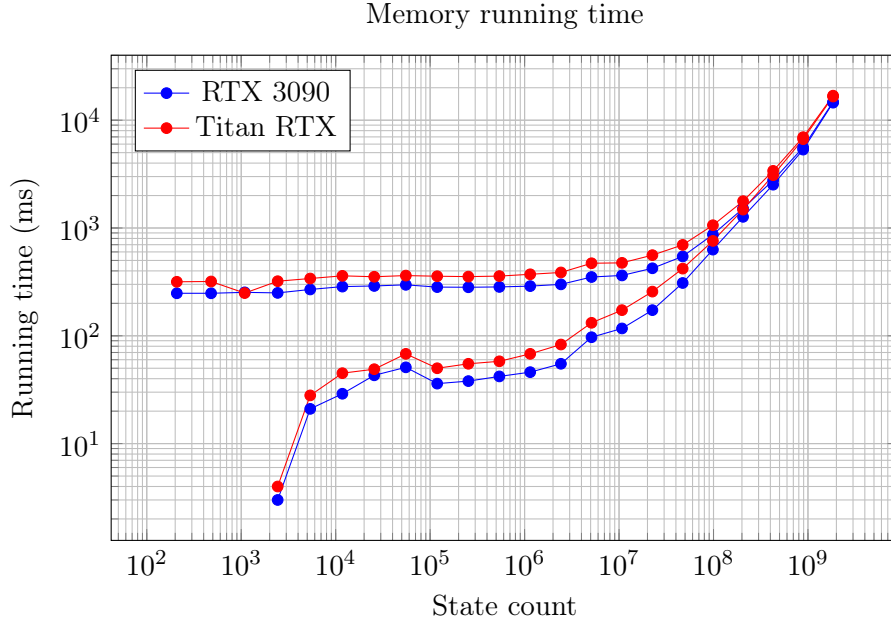
the overall running times from the graph. We were not able to perform inclusion checking for larger DFAs as our GPUs ran out of memory in those cases.

6. CONCLUSIONS & FUTURE WORK

We implemented and compared different parallel algorithms for DFA minimisation on GPUs. We find that the *NC* algorithm **trans** with parallel logarithmic run-time does not scale well because of the large number of resources needed. Instead, we find that the partition refinement algorithms perform better. This might be seen as contradictory since these partition refinement algorithms have inherently linear parallel run-times.

When comparing the different partition refinement algorithms, the structure of the input DFA is of high influence. The trade-off is that in **sortPR** each iteration takes more time than in **naivePR**, but in **sortPR**, an iteration has the potential to lead to a block being split into more than two subblocks. When this happens sufficiently often, fewer iterations are needed.

Name	Benchmark metrics	RTX 3090 Times (ms)			Titan RTX Times (ms)		
	State count	Total	Initial	Exploration	Total	Initial	Exploration
memory.5	88	301	301	0	448	448	0
memory.6	208	248	248	0	317	317	0
memory.7	480	248	248	0	319	319	0
memory.8	1,088	253	253	0	249	249	0
memory.9	2,432	250	246	3	321	317	4
memory.10	5,376	269	249	21	340	313	28
memory.11	11,776	286	257	29	360	314	45
memory.12	25,600	290	247	43	353	304	49
memory.13	55,296	297	247	51	362	294	68
memory.14	118,784	283	247	36	357	307	50
memory.15	253,952	282	244	38	354	300	55
memory.16	540,672	284	242	42	358	300	58
memory.17	1,146,880	289	243	46	372	304	68
memory.18	2,424,832	300	244	55	387	305	83
memory.19	5,111,808	351	254	97	471	339	132
memory.20	10,747,904	363	246	117	475	302	173
memory.21	22,544,384	423	250	173	560	302	257
memory.22	47,185,920	545	235	309	697	278	420
memory.23	98,566,144	869	239	630	1,061	302	759
memory.24	205,520,896	1,518	248	1,269	1,775	294	1,481
memory.25	427,819,008	2,771	249	2,522	3,389	299	3,090
memory.26	889,192,448	5,586	251	5,335	6,957	289	6,668
memory.27	1,845,493,760	14,791	251	14,539	16,892	307	16,584

Table 5: Results of running GPUEXPLORE inclusion checking on **memory** instances.Figure 10: Exploration time and total time for different configurations of **memory**, ranging from $n = 5$ up to and including $n = 27$. The total time includes the initialisation time of the CUDA context.

This leads to **sortPR** being slower in cases where the number of iterations is high. In other benchmarks, it leads to fewer iterations and thereby a significant speed-up.

Finally, we showed a way to incorporate a partial transitive closure in partition refinement algorithms. We showed that for a specific class of DFAs this approach leads to logarithmic run-times, where every partition refinement algorithm is inherently linear.

Regarding equivalence and inclusion checking, we proposed a way to perform a naive variant of the Hopcroft-Karp algorithm massively parallel on a GPU, by encoding these problems in SLCO, an input language of the GPU-accelerated explicit-state model checking GPUEXPLORE. We presented several benchmarks, and demonstrated that for multiple of these, an almost linear increase of the overall execution time can be observed, meaning that the lack of a union-find data structure, which is used in the original Hopcroft-Karp algorithm, is largely mitigated by the use of parallelism.

As future work it would be interesting to further investigate sublinear time parallel algorithms for DFA minimisation. Specifically, there are two key questions that come to mind. The first question is: what is a reasonable number of parallel processes necessary for a poly-logarithmic time parallel algorithm? It seems feasible to use a similar argument as in [KV94] to get a superlinear lower bound. However, the gap between the $O(n^{2\omega})$ processors³ used in Algorithm 1 remains large. The second question is: can a method such as the one presented in this paper using the partial transitive closure be implemented in such a way that the run time will be sublinear with high probability, i.e. any parallel run-time $O(n^{1-\epsilon})$ for some $\epsilon \geq 0$. A good starting point would be the recent work on parallel reachability algorithms [UY90, Fin18, JLS19].

Interesting future work for equivalence and inclusion checking would be to consider the union-find data structure used in the Hopcroft-Karp algorithm to achieve a near-linear complexity. If a massively parallel version of such a data structure can be designed, it can be expected that the execution times of our GPU approach will improve. However, to what extent it will improve in practice will require further experimentation.

³If matrix multiplication can be computed in time $O(n^\omega)$, currently best known bounds $\omega \leq 2.372\dots$

REFERENCES

- [AAP⁺23] Muhammad A. Awad, Saman Ashkiani, Serban D. Porumbescu, Martin Farach-Colton, and John D. Owens. Analyzing and Implementing GPU Hash Tables. In *APOCS*. SIAM, 2023.
- [AHU74] A.V. Aho, J.E. Hopcroft, and J.D. Ullman. *The Design and Analysis of Computer Algorithms*. Addison-Wesley, 1974.
- [BGS92] J. Balcázar, J. Gabarro, and M. Santha. Deciding bisimilarity is P-complete. *Formal aspects of computing*, 4(1):638–648, 1992. doi:10.1007/BF03180566.
- [BH12] N. Bell and J. Hoberock. Thrust: A Productivity-Oriented Library for CUDA. In *GPU Computing Gems Jade Edition*, chapter 26, pages 359–371. Morgan Kaufmann Publishers Inc., 2012. doi:10.1016/C2010-0-68654-8.
- [CH92] S. Cho and D.T. Huynh. The parallel complexity of coarsest set partition problems. *Information Processing Letters*, 42(2):89–94, 1992. doi:10.1016/0020-0190(92)90095-D.
- [CRS08] G. Castiglione, A. Restivo, and M. Sciortino. Hopcroft’s algorithm and cyclic automata. In C. Martín-Vide, F. Otto, and H. Fernau, editors, *Proc. of LATA 2008*, volume 5196 of *LNCS*, pages 172–183. Springer, 2008. doi:10.1007/978-3-540-88282-4_17.
- [dPWZ18] S.M.J. de Putter, A.J. Wijs, and D. Zhang. The SLCO Framework for Verified, Model-driven Construction of Component Software. In *FACS*, volume 11222 of *LNCS*, pages 288–296. Springer, 2018. doi:10.1007/978-3-030-02146-7_15.
- [Eng12] L.J.P. Engelen. *From Napkin Sketches to Reliable Software*. PhD thesis, Eindhoven University of Technology, 2012.
- [Fin18] J.T. Fineman. Nearly work-efficient parallel algorithm for digraph reachability. In *Proc. of STOC 2018*, pages 457–470. ACM, 2018. doi:10.1145/3188745.3188926.
- [GMdV23] J.F. Groote, J.J.M. Martens, and E.P. de Vink. Lowerbounds for bisimulation by partition refinement. *Logical Methods in Computer Science*, Volume 19, Issue 2, May 2023. doi:10.46298/lmcs-19(2:10)2023.
- [HJ86] W.D. Hillis and G.L. Steele Jr. Data parallel algorithms. *Communications of the ACM*, 29(12):1170–1183, 1986. doi:10.1145/7902.7903.
- [HK71] J.E. Hopcroft and R.M. Karp. A linear algorithm for testing equivalence of finite automata. Technical report 114, Cornell University, 1971.
- [Hop71] J. Hopcroft. An $n \log n$ algorithm for minimizing states in a finite automaton. In Z. Kohavi and A. Paz, editors, *Theory of Machines and Computations*, pages 189–196. Academic Press, 1971. doi:10.1016/b978-0-12-417750-5.50022-1.
- [HWWL24] S. Hegeman, D. Wöltgens, A.J. Wijs, and A. Laarman. Compact Parallel Hash Tables on the GPU. In *Proc. 30th European Conference on Parallel and Distributed Processing (Euro-Par 2024)*, Part II, volume 14802 of *LNCS*, pages 226–241. Springer, 2024. doi:10.1007/978-3-031-69766-1_16.
- [J92] J. JáJá. *An introduction to parallel algorithms*. Addison Wesley Longman Publishing Co., Inc., USA, 1992.
- [JLS19] A. Jambulapati, Y.P. Liu, and A. Sidford. Parallel reachability in almost linear work and square root depth. In *Proc. of FOCS 2019*, pages 1664–1686. IEEE, 2019. doi:10.1109/FOCS.2019.00098.
- [KV94] S. Khuller and U. Vishkin. On the parallel complexity of digraph reachability. *Information Processing Letters*, 52(5):239–241, 1994. doi:10.1016/0020-0190(94)00153-7.
- [Les19] B. Lessley. Data-Parallel Hashing Techniques for GPU Architectures. *IEEE Trans. Parallel Distributed Syst.*, 31(1):237–250, 2019. doi:10.1109/TPDS.2019.2929768.
- [MGH⁺22] J.J.M. Martens, J.F. Groote, L.B. Haak, P. Hijma, and A.J. Wijs. Linear parallel algorithms to compute strong and branching bisimilarity. *Software and Systems Modeling*, pages 1–25, 2022. doi:10.1007/s10270-022-01060-7.
- [Moo56] E.F. Moore. Gedanken-experiments on sequential machines. In Claude Shannon and John McCarthy, editors, *Automata Studies*, pages 129–153. Princeton University Press, Princeton, NJ, 1956. doi:10.1515/9781400882618-006.
- [MW24] J.J.M. Martens and A.J. Wijs. An Evaluation of Massively Parallel Algorithms for DFA Minimization. In *Proc. 15th International Symposium on Games, Automata, Logics, and Formal Verification (GandALF 2024)*, volume 409 of *EPTCS*, pages 138–153. Open Publishing Association, 2024.

- [OW24] M. Osama and A.J. Wijs. Hitching a Ride to a Lasso: Massively Parallel On-The-Fly LTL Model Checking. In *Proc. 30th International Conference on Tools and Algorithms for the Construction and Analysis of Systems (TACAS 2024), Part II*, volume 14571 of *LNCS*, pages 23–43. Springer, 2024. doi:10.1007/978-3-031-57249-4_2.
- [PT87] R. Paige and R. E. Tarjan. Three partition refinement algorithms. *SIAM Journal on Computing*, 16(6):973–989, 1987. doi:10.1137/0216062.
- [RS59] M.O. Rabin and D. Scott. Finite automata and their decision problems. *IBM Journal of Research and Development*, 3(2):114–125, 1959. doi:10.1147/rd.32.0114.
- [RX96] B. Ravikumar and X. Xiong. A parallel algorithm for minimization of finite automata. In *Proceedings of the 10th International Parallel Processing Symposium, IPPS '96*, pages 187–191, USA, 1996. IEEE Computer Society. doi:10.1109/IPPS.1996.508056.
- [SV84] L. Stockmeyer and U. Vishkin. Simulation of parallel random access machines by circuits. *SIAM Journal on Computing*, 13(2):409–422, 1984. doi:10.1137/0213027.
- [TB73] B.A. Trakhtenbrot and J.M. Barzdin. *Finite automata: behavior and synthesis*. North-Holland Publishing, 1973.
- [TSG02] A. Tewari, U. Srivastava, and P. Gupta. A parallel DFA minimization algorithm. In *Proc. of HiPC*, volume 2552 of *LNCS*, pages 34–40. Springer, 2002. doi:10.1007/3-540-36265-7_4.
- [UY90] J. Ullman and M. Yannakakis. High-probability parallel transitive closure algorithms. In *Proc. of SPAA 1990*, pages 200–209, 1990. doi:10.1145/97444.97686.
- [WB14] Anton Wijs and Dragan Bošnački. GPUexplore: Many-Core On-the-Fly State Space Exploration Using GPUs. In *Proc. 20th International Conference on Tools and Algorithms for the Construction and Analysis of Systems (TACAS 2014)*, volume 8413 of *LNCS*, pages 233–247, 2014. doi:10.1007/978-3-642-54862-8_16.
- [WB16] Anton Wijs and Dragan Bošnački. Many-Core On-The-Fly Model Checking of Safety Properties Using GPUs. *STTT*, 18(2):169–185, 2016. doi:10.1007/s10009-015-0379-9.
- [Wij15] A.J. Wijs. GPU accelerated strong and branching bisimilarity checking. In C. Baier and C. Tinelli, editors, *Proc. of TACAS*, volume 9035 of *LNCS*, pages 368–383. Springer, 2015. doi:10.1007/978-3-662-46681-0_29.
- [Wij23] A.J. Wijs. Embedding Formal Verification in Model-Driven Software Engineering with SLCO: An Overview. In *Proc. 19th International Conference on Formal Aspects of Component Software (FACS 2023)*, volume 14485 of *LNCS*, pages 206–227. Springer, 2023.
- [WNB16] Anton Wijs, Thomas Neele, and Dragan Bošnački. GPUexplore 2.0: Unleashing GPU Explicit-State Model Checking. In *Proc. 20th International Symposium on Formal Methods (FM 2016)*, volume 9995 of *LNCS*, pages 694–701. Springer, 2016. doi:10.1007/978-3-319-48989-6_42.
- [WO23a] A.J. Wijs and M. Osama. GPUEXPLORE 3.0: GPU Accelerated State Space Exploration for Concurrent Systems with Data. In *Proc. 29th International Symposium on Model Checking Software (SPIN 2023)*, volume 13872 of *LNCS*, pages 188–197. Springer, 2023. doi:10.1007/978-3-031-32157-3.
- [WO23b] A.J. Wijs and M. Osama. A GPU Tree Database for Many-Core Explicit State Space Exploration. In *Proc. 29th International Conference on Tools and Algorithms for the Construction and Analysis of Systems (TACAS 2023), Part I*, volume 13993 of *LNCS*, pages 684–703. Springer, 2023. doi:10.1007/978-3-031-30823-9_35.
- [WO24] A.J. Wijs and M. Osama. The fast and the capacious: memory-efficient multi-GPU accelerated explicit state space exploration with GPUexplore 3.0. *Frontiers in High Performance Computing*, 2, 2024. doi:10.3389/fhpcp.2024.1285349.